

Dependence of Coefficient of volumetric thermal expansion (CVTE) of glass fiber reinforced (GFR) polymers on the glass fiber content

V. La Carrubba^(a) (✉), M. Bulters^(b), W. Zoetelief^(b)

^(a) Chemical Engineering Department, University of Palermo - Viale delle Scienze, 90128 Palermo, Italy

^(b) DSM Research - P.O. Box 18, 6160 MD, Geleen, The Netherlands

E-mail: lacarrubba@dicpm.unipa.it; Fax: +39-091-6567280

Received: 15 December 2006 / Revised version: 19 July 2007 / Accepted: 12 August 2007
Published online: 25 August 2007 – © Springer-Verlag 2007

Summary

In a Glass Fiber Reinforced (GFR) polymer, the coefficient of volumetric thermal expansion CVTE (determined as a sum of the coefficients of linear thermal expansion CLTE's for the three principal directions) is sometimes much smaller than the value predictable on the basis of well acquainted models, such as Chow model, taking into account fibers anisotropy and aspect ratio.

A detailed investigation of the CVTE of unfilled and GFR thermoplastics (polyethyleneterephthalate PET, polybutyleneterephthalate PBT, polyamide 6 PA6, polyamide 4,6 PA46, polycarbonate PC) was performed through Pressure-Volume Temperature (PVT) measurements. In particular, it was found that CVTE is always much lower than the zeroth order “expected value”, defined according to the “rule of mixture”. The aspect ratio plays a major role, since in the case of polymers filled with glass spheres the rules of mixtures applies for the resulting CVTE. Finally, the nature of the matrix is of paramount importance: a GFR polymer with an amorphous matrix (PC) strictly follows the rule of mixture for CLVE even for highly anisotropic fillers exhibiting large aspect ratios (20 to 30).

1 Introduction and background

A major issue for polymers in engineering applications is to reduce the thermal expansion coefficient so as to achieve dimensional stability more comparable to metals. Numerous studies have examined how filler shape, size, and volume fraction influence the thermal expansion of polymer composites. Long fiber composites have a significantly lower linear thermal expansion coefficient than the matrix polymer [1]. Anisotropic thermal expansion behavior for injection-molded specimens has been observed, the expansion coefficient in the flow direction (FD) being lower than in the perpendicular direction [2, 3].

Filler geometry can also greatly affect physical proper-ties of composites; e.g. high aspect ratios normally contribute to greater reduction in thermal expansion [4].

Enhancement of dimensional stability is expected when a filler with high modulus and low thermal expansion coefficient is dispersed in a matrix of lower modulus and higher thermal expansion coefficient owing to simple mechanical restraints.

Last but not least, an accurate knowledge and prediction of thermal expansion coefficients (hence shrinkage) across different directions in both unfilled and glass filled injection molded samples is a crucial point for an effective prevention of warpage occurrence, often due to asymmetric shrinkage and/or shrinkage differences in different directions (orientation shrinkage) [5].

The linear thermal expansion coefficient along a direction l is defined as:

$$\alpha_l = 1/l \times \partial l / \partial T = \partial \ln(l) / \partial T \quad (1)$$

being l sample length. The volumetric thermal expansion coefficient is defined as:

$$\alpha_v = 1/v \times \partial v / \partial T = \partial \ln(v) / \partial T \quad (2)$$

where v is the specific volume.

In a homogeneous material the relationship between the two coefficients of thermal expansion is such that $\alpha_v = \alpha_x + \alpha_y + \alpha_z$, where x , y and z are three mutually orthogonal directions; obviously in case of an isotropic material $\alpha_v = 3\alpha_l$.

In a Glass Fiber Reinforced (GFR) polymer, the thermal expansion coefficient may be expected to result from the rule of mixtures; the contribution of the thermal expansion of the polymer matrix (α_p) and the filler (α_g), are weighed by their respective volumetric fractions f [6]:

$$\alpha_{GFR} = \alpha_p f_p + \alpha_g (1 - f_p) \quad (3)$$

More refined models, such as the Chow model [7], or the Schapery model [8] take into account the filler anisotropy and aspect ratio (through the deformation state).

The presence of large aspect ratio fillers, like fibers, induces mechanical constraints on the polymer matrix resulting in a lower “effective” coefficient of volumetric thermal expansion α_v , depending on several factors: the nature of the polymer matrix, the fiber distribution and hence the inter-fiber distance, and the matrix/fiber adhesion. Recent work on Polyamide 6 nanocomposites [9] has shown that the α_v of these systems (determined as a sum of the Coefficients of Linear Thermal Expansion in the three principal directions) is sometimes much smaller than the value predicted by these models. However, the use of more accurate closure approximations applied to the Tucker-Liang [10] and Mori-Tanaka [11-12] model have notably improved the evaluation of thermoelastic properties of injection molded short-fiber composites [13]. The purpose of the present experimental work was to determine and compare the α_v of unfilled (UF) and GFR crystalline (poly-ethylene-terephthalate PET, poly-buthylene-terephthalate PBT, polyamide-6 PA6, polyamide-4,6 PA46) and amorphous thermoplastics (polycarbonate PC), in order to validate the proposed models [7-9] and to highlight the dependence of this coefficient upon the volumetric filler content. Furthermore the influence of fiber aspect ratio and of the nature of the matrix (amorphous vs. semicrystalline) is presented and shortly discussed.

2 Experimental

Volumetric coefficients of Expansion were determined through Pressure-Volume Temperature (PVT) analysis. The apparatus used was the “Gnomix PVT”, based on

the use of a confining fluid and a special “sample cup”, ensuring a hydrostatic state of stress (i.e. a true pressure) in the sample at all times and phases [14].

Linear thermal expansion coefficients across directions perpendicular and parallel to flow were measured by means of a standard apparatus according to ASTM E831.

Rectangular plates 800 mm long, 500 mm wide and 1.5 mm thick were injection moulded in a mould plate with a sprue gate positioned in the centre (see fig. 1) by using standard injection moulding conditions. Materials and compositions as reported in table 1. Standard short glass fibers approximately 300 μm long with an L/D ranging from 10 to 15 were compounded in different proportions with different polymeric matrices, including both semicrystalline (PET, PBT, PA46 and PA6) and amorphous polymers (PC). In one case (PA6) glass beads with a diameter of approximately 30 μm were compounded (see Table 1).

Three injection molded samples per each material composition were taken for the experimental investigations (PVT and Linear Expansion runs).

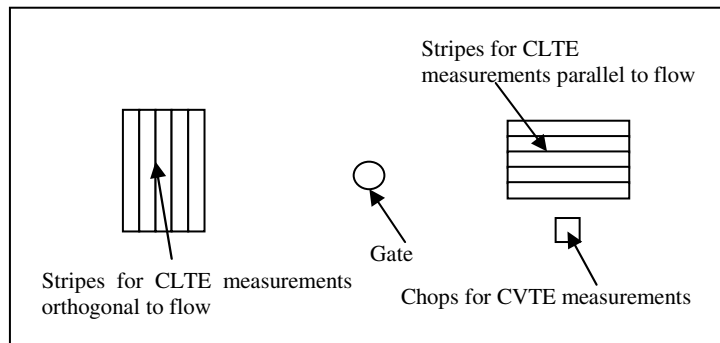


Figure 1: Schematic of the mould plate geometry, indicating samples used for CLTE and CVTE

Table 1: Materials analyzed

Material	Glass fiber content, wt %
PET	0, 50
PBT	0, 35
PA46	0, 60
PA6	0, 50, 50 (glass beads)
PC	0, 30

For the linear thermal expansion measurements 5 rectangular stripes 100 mm long and 20 mm wide were cut across directions perpendicular and parallel to flow, as schematically shown in fig. 1. The stripe length as a function of time was monitored by means of a LINSEIS 8 push-rod Dilatometer type L75/120-LT from 120 to -15°C ; 5 samples were measured per material. Typical examples of the raw data, showing averaged ΔL as a function of temperature for PA46-uF samples cut across parallel and perpendicular direction are reported in fig. 2.a and b respectively.

On the other hand, samples of 1.2 to 1.5 g were taken from the plate zones with fully developed flow (hence reasonably characterized by the largest fiber orientations), i.e. in between the gate and the plate edges but sufficiently far from both (see fig. 1), in order to investigate the dependence of α_V upon the nature of the matrix, the presence

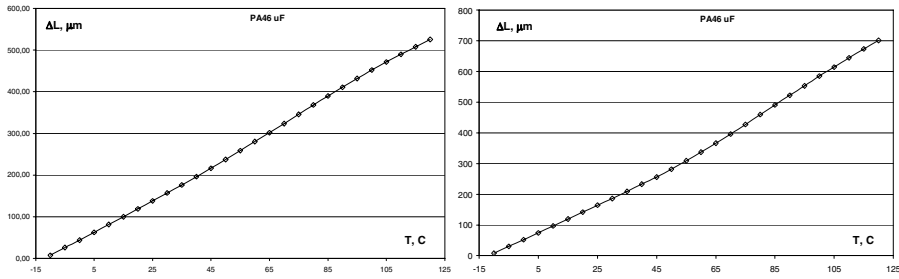


Figure 2: ΔL vs. temperature as recorded by the apparatus for measuring α_l . a (left): PA46-uF parallel direction. B (right): PA46-uF perpendicular direction)

of glass fibers, and their aspect ratio. However, the orientation distribution across the plate thickness was not examined, going beyond the scope of the present investigation, aiming to provide easy-to-handle correlations among the thermal expansion behavior and the volumetric fiber content in short fiber polymer composites.

These samples were subjected to successive isothermal compressions from 30 to 60°C, at subsequent pressures ranging from 10 to 200 MPa at intervals of 10 MPa. From these data α_v was calculated. As an example, fig. 3.a shows the dependence of specific volume upon temperature in the range from 30 to 60°C for the PBT GFR sample. It is opportune to recall that the curve at ambient pressure is automatically provided by the software of the PVT instrument via extrapolation of higher pressure data [14]. The thermal expansion coefficient is determined from the slope of the plot of $\ln(v)$ versus temperature, see eq (2), as schematically shown in fig. 3.b for a PBT-GFR and a PA6 uF at different pressure values.

Finite Element (FE) simulations of the stress state on a single glass fiber surrounded by a polymer matrix (volumetric fiber content of 25%) were carried out with the help of the MSC-MARC software. A pure isotropic elastic behavior was assumed as a first order approximation with periodic boundary conditions (for the displacements), and

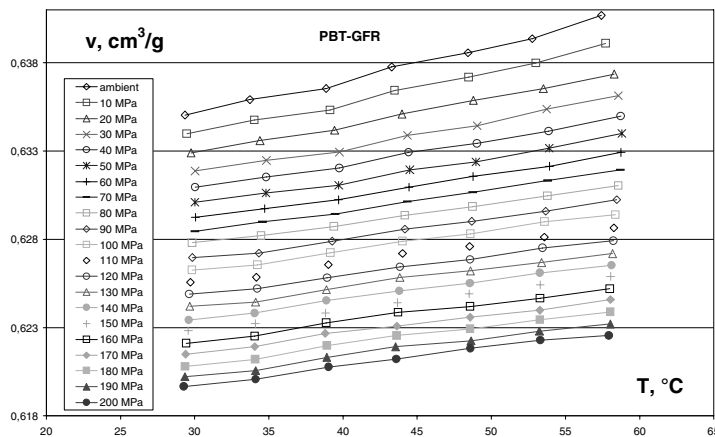


Figure 3.a: Specific volume vs. T for different pressures

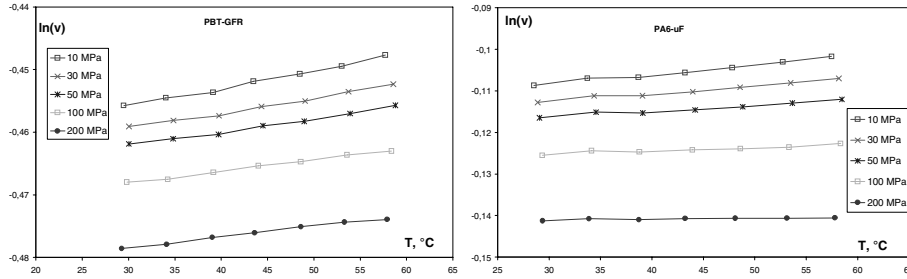


Figure 3.b: Log of specific volume vs. T for different pressures. Left: PBT-GFR; right: PA6 uF

a cooling step of 50°C (“shrinkage load”) down to room temperature was examined, reporting the results in terms of equivalent von Mises’ iso-stress curves (being the frozen stresses generated by the thermal contraction owing to cooling).

3 Results and discussion

For all the materials investigated in this (narrow) temperature range, α_V turns out to be constant with temperature, and decreases with pressure, see figures 4 to 8.

Results for the unfilled (UF) PBT and the PBT/GFR are presented in fig. 4, which shows that α_V is strongly reduced by the presence of the glass fibers. The actual value of α_V , over the whole pressure range, of the glass filled samples is some 25-30% lower than calculated through eq (3), i.e. by a mere volumetric weighed average of the α_V ’s of the pure polymer and of the glass (see triangles in fig. 4). The volumetric content was calculated based on the average matrix density (measured in the PVT at different pressures), on the glass fiber density and on the particular weight fraction. The compressibility of glass may be found in literature [15], its value being definitely negligible with respect to the typical compressibility of a polymer matrix in the explored pressure range (maximum pressure 200 MPa). The decrease of α_V with respect to the “rule of mixtures” value predicted by several models (see for instance the Chow model) is less than 10% for 25% glass fiber volumetric content and a fiber aspect ratio of 10 [7]. As a matter of fact, according to the Chow model, the thermal expansion coefficient of a GFR polymer may be calculated by:

$$\alpha_{GFR} = \alpha_p + (k_g / k_m) \times (\alpha_g - \alpha_p) (G_1 + 2G_3) \phi / (2K_1G_3 + G_1K_3) \quad (4)$$

where k_i are the bulk moduli, ϕ is the volumetric fiber content and K_i , G_i are coefficients depending on the Poisson’s ratio of the polymer and on the aspect ratio of the glass. It may be easily shown [7] that eq (4) does not supply values significantly deviating from the values given by eq (3): this is visibly shown in fig. 4, where the predictions of the volumetric thermal expansion according to the Chow Model are reported, almost coinciding with the values provided by the rule of mixtures.

The deviation between measured and expected values (based on the rule of mixtures) is even more pronounced in the case of the PA46 and PA46-GFR, as shown in fig. 5. A slightly different behavior is exhibited by PET-based systems (fig. 6), where the α_V of PET-GFR is much less dependent on pressure. It is also worthwhile noticing that the absolute value of α_V ’s of the PET-based systems (ranging from 1.2e to 2.3*10⁻⁴) is much lower than the one of the PBT-based systems (from 1.7 to 3.5*10⁻⁴).

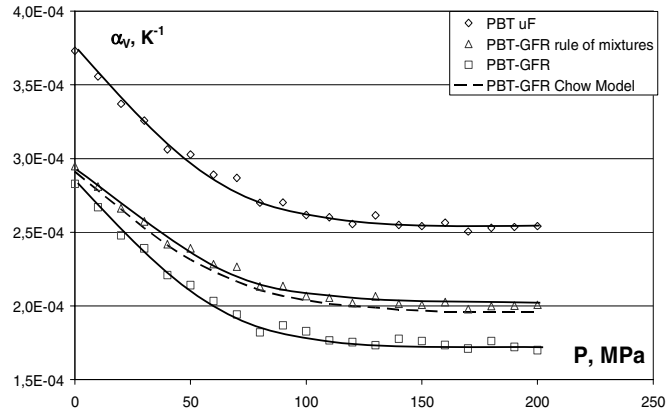


Figure 4: α_v for PBT: UF, GFR, eq (2) and Chow Model (eq 4)

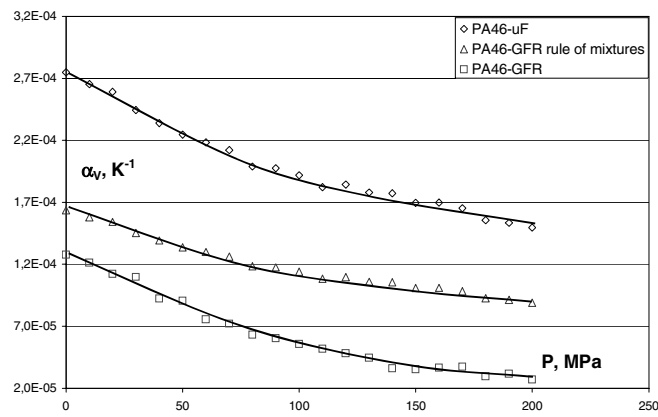


Figure 5: α_v for PA46: UF, GFR and eq (2)

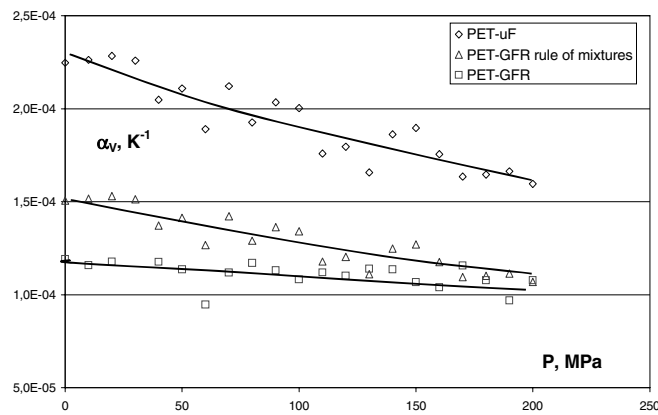


Figure 6: α_v for PET: UF, GFR and eq (2)

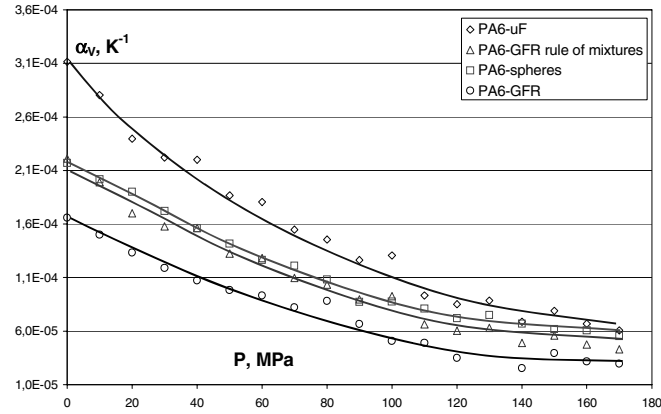


Figure 7: α_v for PA6: UF, GFR, spheres and eq (2)

That the aspect ratio of the filler affects the expansivity is illustrated in fig. 7, where α_v 's for UF PA6 and for PA6 filled with equal volumetric content of glass fibers and glass beads (aspect ratio equal to one), respectively, are compared.

While in the case of GFR PA6 the behavior is in line with the one exhibited by the other systems whose matrix is a semicrystalline polymer, in the case of PA6 filled with glass spheres the measured values of α_v almost coincide with the one predicted by the rule of mixtures (eq.3). An increase of the aspect ratio from 1 (spheres) to about 30 (the typical aspect ratio of the fibers used in glass fiber filled systems) corresponds to a relative decrease in the thermal expansion coefficient of about 25%.

Finally, α_v as a function of pressure for the PC-UF and the PC-GFR are reported in fig. 8. Like in the case of PA6 filled with glass spheres, the measured values of the thermal expansion coefficient do follow the rule of mixtures over the whole pressure range, showing that also the matrix properties are relevant.

Another interesting heuristic conclusion can be drawn by defining the “excess normalized coefficient of thermal expansion” $\alpha_{e,n}$ as follows:

$$\Gamma_{e,n} = (\alpha_{rom} - \alpha_{meas}) / \alpha_{rom} \quad (5)$$

expressing the deviation of the experimentally measured thermal expansion α_{meas} from the “reference value”, α_{rom} , which is the expected value of expansivity calculated using the rule of mixtures (eq.3). Although both α_{meas} and α_{rom} exhibit a significant dependence upon pressure (at least up to 100 MPa), however their difference (normalized by α_{rom}) shows only a mild dependence upon pressure, therefore the average value of $\Gamma_{e,n}$ in the range 0-50 MPa (the typical span of pressure values normally employed in polymer processing) will be reported in the following for each material.

This parameter indicates how large the departure of α_v is from “ideality” (the rule of mixtures). Fig. 9 reports $\Gamma_{e,n}$ as a function of the volumetric fiber content.

It should be noticed that all points align quite well on a straight line passing through the origin, indicating the existence of a correlation between the volumetric fiber glass content and the decrease of α_v with respect to the “expected” value. It is worth stressing that the data refer to 4 different materials (PET, PBT, PA6 and PA46).

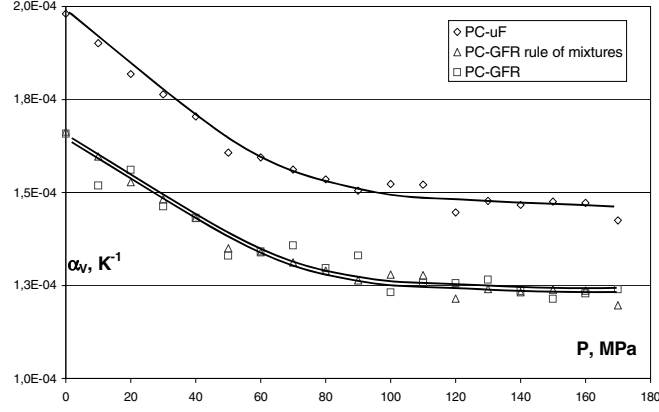


Figure 8: α_v for PC: UF, GFR and eq (2)

In other words, the presence of glass fibers exerts a significant constraint on the surrounding polymeric material, hindering its expansion and hence lowering its α_v . This constraining action is almost independent of the nature of the matrix (if semicrystalline), at least for the polymers studied in this experimental campaign.

Furthermore, the results of fig. 9 may provide some quantitative information about this “constraining effect”. As a matter of fact, the slope of the curve is equal to 0.6, which means that the presence of fibers determines a further decrease of the volumetric thermal expansion coefficient with respect to the one determined on the basis of a volumetric additivity, see eq (3), this decrease being equivalent to an “effective” glass fiber content approximately equal to a 60% increase with respect to the real content. More exactly, since

$$(\alpha_{rom} - \alpha_{meas}) / \alpha_{rom} = 0.6 \times f_g \quad (6)$$

where f_g is the volumetric fiber fraction, and since

$$\alpha_{rom} = \alpha_p \times (1 - f_g) + \alpha_g \times f_g \quad (7)$$

one can calculate an “equivalent” volumetric glass fiber fraction f_g^* , defined as:

$$\alpha_{meas} = \alpha_p \times (1 - f_g^*) + \alpha_g \times f_g^* \quad (8)$$

or, equivalently:

$$f_g^* = (\alpha_p - \alpha_{meas}) / (\alpha_p - \alpha_g) \quad (9)$$

From eqs (6) (7) and (9) the relationship between f_g^* and f_g can be found:

$$f_g^* / f_g = (1 + 0.6 f_g) + 0.6 \alpha_p / (\alpha_p - \alpha_g) \quad (10)$$

Since for all polymers it is easy to notice that $\alpha_p \gg \alpha_g$, one may write with a good approximation:

$$f_g^* / f_g \approx 1.6 + 0.6 \times f_g \quad (11)$$

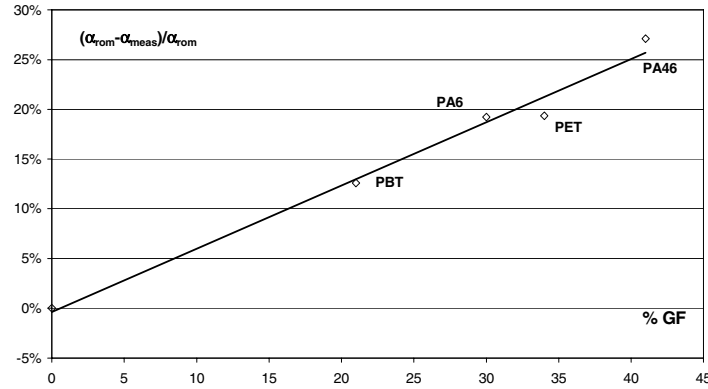


Figure 9: Excess normalized α_V vs. vol. fiber content

Therefore, if one wants to determine the volumetric thermal expansion coefficient, the real glass fiber content must be multiplied by a factor reported in eq.10. In volumetric terms this means that a portion of polymer around the fiber larger than 60% of the real fiber volume is hindered in the expansion, with the ratio between the “effective” fiber diameter D_{eff} and the real fiber diameter D equal to:

$$D_{eff} / D \approx \sqrt{1.6 + 0.6 \times f_g} \quad (12)$$

In order to verify the reasonability of the hypothesis of an “effective” fiber diameter resulting from a compressive state around the fiber, Finite Element (FE) simulations of the stress state on a single fiber surrounded by a PET matrix were carried out (by using the program MSC-MARC). A cooling step of 50°C (“shrinkage load”) in the solid state (down to room temperature) was simulated and the resulting stress state around glass fibers (in terms of equivalent von Mises’ stresses) is reported in fig. 10, which shows that an “effective fiber diameter” exists (larger than the geometrical one), whose extent depends upon the definition of a “critical von Mises’ stress” above which an effective constraining effect takes place (around 10% more of the geometrical diameter for a critical value of 100 MPa and around 30% for a critical value of 70 MPa).

In other words, a “stress-confined” region around a glass fiber exists, where the volumetric expansion is hindered owing the frozen-in thermal stresses, the final outcome being a net reduction in the volumetric coefficient of thermal expansion, which turns out to be lower than the “expected” value, evaluated according to the rule of mixtures (eq 3).

Similar consideration could be made by looking at the first invariant of the stress tensor, whose contour maps are not reported here for the sake of brevity.

On the other hand, when the matrix is amorphous (PC, see fig. 8) or the fiber aspect ratio tends to 1 (PA6 filled with glass spheres, see fig. 7), the excess normalized α_V is always zero, regardless the glass fiber content. The experimental evidence concerning GFR polymers (PC) however deserves further investigations.

In particular, the larger “effective” fiber diameter (experimentally determined) noticeable in various type of semicrystalline polymers (polyesters and polyamides), suggests the hypothesis of a possible additional contribution of the nucleating effect exerted by the glass fiber onto the surrounding semicrystalline polymer matrix (and

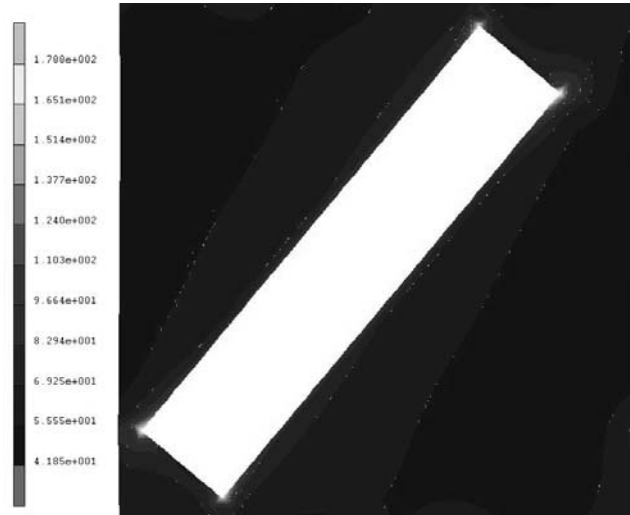


Figure 10: FE equivalent von Mises' Stress for volumetric expansion of a PET matrix around a single glass fiber. Matrix properties: $E=3.5$ GPa, $\nu=0.394$, $CLTE = 2.5 \cdot 10^{-4}$ [1/K]; fiber properties: $E = 70$ GPa, $\nu=0.18$, $CLTE \approx 0$ [1/K]

not onto an amorphous matrix). Although this argument sounds reasonable, since it has been frequently observed in polyolefinic matrices (iPP), so-far the experimental evidences concerning polyesters are not supporting it [16].

In any case, the experimental evidence corroborates the hypothesis that the reduction of the thermal expansion coefficient is related to the interplay between the constraining effect induced by the stress state and the specific polymer morphology around the glass fiber.

Coefficients of linear expansion α_l across directions perpendicular and parallel to flow were measured by taking the slope of $\ln(L)$ vs. T curve (see eq.1). By plotting α_l versus α_v for the all the unfilled materials one gets the data reported in fig. 11. α_l across parallel and perpendicular direction were measured by the linear thermal

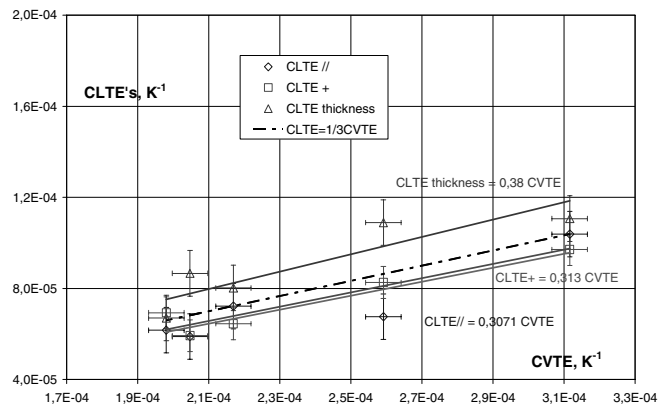


Figure 11: CLTE's versus CVTE for unfilled materials

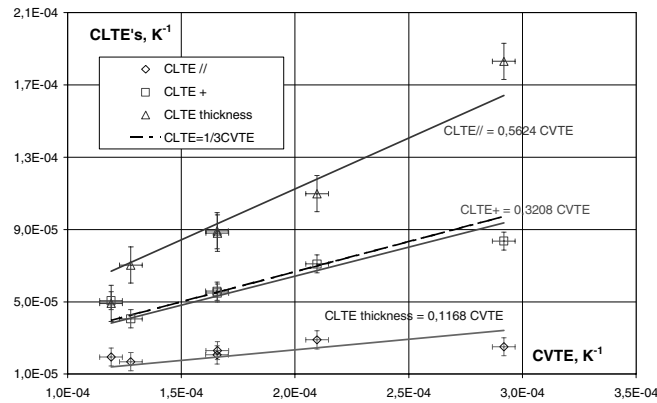


Figure 12: CLTE's versus CVTE for GFR materials

expansion coefficient apparatus, α_V values come from the PVT data at ambient pressure and α_l across the thickness direction is obtained by subtracting from α_V the value of α_l parallel and α_l perpendicular. It is easy to notice that the three coefficients do not significantly differ from each other; additionally, the slope of all the curves is very close to 1/3, rigorously valid for isotropic materials. The final conclusion is that for unfilled materials there is not a significant thermal anisotropy.

When iterating the same procedure for glass fiber reinforced materials, the data reported in fig. 12 are obtained. In this case a large thermo-mechanical anisotropy should be noticed, i.e. both an “intrinsic” anisotropy in thermal properties and an induced” anisotropy due to the thermal history experienced during processing. As a consequence of that the coefficient along parallel direction turns out to be very small, the one across perpendicular direction is close to 1/3 and the one across thickness direction is about 2/3.

4 Conclusions

The large set of obtained experimental data concerning the coefficients of thermal expansion (volumetric and linear) leads to the following main conclusions:

- the experimentally determined value of volumetric thermal expansion for semicrystalline polymers (polyamides and polyesters) filled with glass fibers is always lower than the “expected value” based on the “rule of mixtures”;
- a synthetic parameter, here named “excess normalized coefficient of thermal expansion” ($\Gamma_{e,n}$), expressing the deviation of the experimentally measured thermal expansion from the “rule-of-mixtures based” expansivity can be suitably applied to describe the observed reduction of the volumetric thermal expansion coefficient;
- in particular, $\alpha_{e,n}$ linearly depends on the glass fiber volumetric content for semicrystalline polymers, whereas one amorphous polymer here tested, PC, behaves differently, since the rule of mixture always applies; this evidence, if confirmed for other composites based on amorphous polymeric matrices, may suggests an interplay between the constraining effect induced by the stress state and the specific polymer morphology around the glass fiber (transcrystalline regions in the vicinity of the fiber surface); further experiments should be however carried out to confirm the hypothesis;

the filler aspect ratio dominates this behavior, since in semicrystalline polymer(s) filled with beads ($L/D=1$) the mixture rules applies;

- in injection molded specimens the coefficients of linear thermal expansion are equal to 1/3 of the volumetric ones for unfilled polymers where no thermal anisotropy can be noticed; whereas for GFR materials, a very large thermo-mechanical anisotropy is observed, the coefficients of thermal expansion across the thickness directions being much larger than the one across perpendicular direction; finally the coefficient of thermal expansion along the flow direction is about 10% of the volumetric one, in line with previously reported results [2, 3].

5 References

1. Segal R (1979) *Pol Eng Sci* 19:365
2. Okada A, Kawasumi M, Usuki A (1990) *Mater Res Soc Symp Proc* 171:45
3. Okada A., Usuki A (1995) *Mater Sci Eng C3*:109
4. Lusi J, Woodhams BT, Xanthos M (1973) *Polym Eng Sci* 13:139
5. Zeng R, Kennedy P, Phan-Thien N, Fan X-J J. (1999) *Non-Newt Fluid Mech* 84:159
6. Papathanasiou TD, Guell DC (1997) *Flow-induced alignment in composite materials*, Woodhead Publishing limited, Cambridge
7. Chow TS (1978) *J Pol Sci Pol Phys* 16:967
8. Schapery RA (1968) *J Compos Mat* 2:380
9. Yoon PJ, Fornes TD, Paul DR (2002) *Polymer* 43:6727
10. Tucker III CL, Liang CL (1999) *Comp Sci Technol* 59:655
11. Mori T, Tanaka K (1973) *Acta Metall* 21:571
12. Benveniste Y (1987) *Mech Mater* 6:147
13. Draya D, Gilorminia P, Régnier G (2007) *Comp Sci and Technol* 67:1601
14. He J, Zoller P (1994) *J Pol Sci Part B Pol Phys* 32:1049
15. Perman, EP, Urry WD (1927) *Proc Phys Soc* 40:186
16. Assouline E, Wachtel E, Grigull S, Lustiger A, Wagner HD, Marom G (2002) *Macrom* 35:403